

Predicting spike protein NTD mutations of SARS-CoV-2 causing immune escape by molecular dynamics simulations

Liping Zhou^{1,2,#}, Leyun Wu^{1,2,#}, Cheng Peng^{1,2}, Yanqing Yang^{1,2}, Yulong Shi^{1,2}, Zhijian Xu^{1,2,*}, Weiliang Zhu^{1,2,*}

¹CAS Key Laboratory of Receptor Research; Drug Discovery and Design Center, Shanghai Institute of Materia Medica, Chinese Academy of Sciences, Shanghai, 201203, China

²School of Pharmacy, University of Chinese Academy of Sciences, No.19A Yuquan Road, Beijing, 100049, PR China

#These authors contributed equally to this work.

*To whom correspondence should be addressed.

E-mail: zjxu@simm.ac.cn (Z.X.), wlzhu@simm.ac.cn (W.Z.).

ORCID:

Zhijian Xu: 0000-0002-3063-8473

Weiliang Zhu: 0000-0001-6699-5299

ABSTRACT

The emergence of coronavirus disease 2019 (COVID-19) pandemic caused by severe acute respiratory syndrome coronavirus 2 (SARS-CoV-2) has been bringing the world to a standstill. Beyond all doubt, the most striking therapeutic target for antibody development is the spike (S) protein on the surface of virus. In contrast with an immunodominant receptor-binding domain (RBD) of the spike protein, little is known about neutralizing antibodies binding mechanisms of N-terminal domain (NTD), let alone the effect of NTD mutation on antibody binding and risk of immune evasion. Employing various computational approaches in this study, we investigated critical residues for NTD-antibody bindings and their detailed mechanism. The results showed that some residues on NTD including Y144, K147, R246 and Y248 are critically involved in the direct interaction of NTD with many monoclonal antibodies (mAbs), indicating that the viruses harboring these residue mutations may have high risk of immune evasion. Binding free energy calculations and the interaction mechanism study revealed that R246I, which is present in Beta (B.1.351) variant, may decrease or even abrogate the efficacies of many antibodies. Therefore, special attention should be paid to the mutations of the 4 residues for future antibody design and development.

Key Words: COVID-19; spike protein; R246I; NTD antibody; MM/GBSA

INTRODUCTION

The coronavirus disease 2019 (COVID-19) pandemic induced by severe acute respiratory syndrome coronavirus 2 (SARS-CoV-2) poses a serious threat to public health with severe socio-economic damage. As of August 2021, there are more than 213 million confirmed cases and about 4.44 million deaths worldwide¹.

The pathogenic agent, namely SARS-CoV-2, is a kind of positive-sense RNA virus, consisting of spike (S) glycoprotein, membrane protein, envelope glycoprotein, lipid bilayer and inner structures². It belongs to the betacoronavirus genus whose family members include Middle East respiratory syndrome coronavirus (MERS-CoV) and SARS-associated coronavirus (SARS-CoV). Similar to the two family members, SARS-CoV-2 infects host cells through S protein which can interact with the angiotensin-converting enzyme 2 (ACE2) entry receptor on host membranes with high affinity³⁻⁴. As a consequence, the S protein becomes the main target of neutralizing antibodies. S1 and S2 subunits are two functional components of the S protein, of which the former (S1) is further divided into receptor-binding domain (RBD) necessary for ACE2 binding, N-terminal domain (NTD) and other domains⁵⁻⁶. So far, plenty of mAbs recognizing RBD have been discovered such as REGN10933⁷, S2M11⁸. Compared with RBD-specific mAbs, a small number of antibodies targeted to NTD have been developed. Nevertheless, it is reported that some NTD-targeting mAbs are capable of neutralizing SARS-CoV-2 infection *in vitro* with high potency⁹⁻¹⁰. For instance, McCallum *et al.* described 41 NTD-specific human mAbs, among which S2X333 neutralized SARS-CoV-2 with an IC₅₀ of 2 ng/mL, on par with the first-rate RBD mAbs S2E12 and S2M11¹¹. Therefore, NTD may be another promising therapeutic target site.

Although prophylactic and/or therapeutic drugs are being developed at an unprecedented pace, it is still unknown when the epidemic will be under effective control all over the world. One of the most crucial reasons is that a larger number of prevalent mutations and deletions in S glycoprotein have emerged since the start of the outbreak and this rapid viral evolution could either facilitate transmissibility, or lead to reduction in protective efficacy of vaccines and mAbs¹²⁻¹⁴. Typically, SARS-CoV-2

Beta (B.1.351/501Y.V2) variant, emerging in late 2020 in Eastern Cape, South Africa (SA), contains 9 S protein mutations including three mutations (K417N, E484K, N501Y) in RBD, a cluster of NTD mutations (*e.g.*, 242-244del & R246I) and so on¹⁵. Wang *et al.* found that this variant is refractory to neutralization by convalescent plasma and vaccine sera¹⁶. McCarthy *et al.* found that 90% of deletion mutations occupied four discrete sites within the NTD¹². What is worth mentioning is that SARS-CoV-2 Lambda (B.1.621) variant, a new variant of interest with higher infectivity and immune resistance, has T76I, L452Q, F490S and a unique 7-amino-acid insertion mutation (RSYLTPGD246-253N) in the N-terminal domain¹⁷. All of above have made the current drug development situation even grimmer. Hence, it matters laying emphasis on immunogenicity of different S protein domains and the specific mechanism of mAbs targeting them, including NTD.

Up to now, there have already been numerous studies to learn the effects and mechanism of mutations in the RBD domain¹⁸⁻²⁰. In particular, RBD mutations containing E484K, N501Y and K417N have attracted considerable attention from researchers²¹⁻²³. Whereas, the details of the NTD mutations have been still elusive until now, owing to the absence of attaching great importance to this antigenic site. When it comes to researches about NTD, recent reports elucidated that several currently circulating variants, comprising Beta (B.1.351) and Alpha (B.1.1.7), harbors some NTD mutations like Y144del, R246I, *etc.*, and these lineages will partially or completely escape neutralization mediated by a variety of mAbs¹⁶. The biochemistry experiments by McCallum and Wang *et al.* both give evidence of some NTD single-point mutations including R246I, R246A, K147T impairing immune therapies^{11, 16}. Kimura *et al.* revealed that the RSYLTPGD246-253N insertion mutation in the N-terminal domain of the Lambda S protein, is responsible for evasion from neutralizing antibodies¹⁷. By comparison, even though A222V possesses a high mutation rate according to statistic by GISAID sequence database²⁴, it makes no difference to immunogenicity¹¹. Considering this, it is of great significance to understand binding modes of NTD antibody-antigen and distinguish detrimental mutations effectively from so much data.

Complementary to time-consuming wet lab study, computational methods are

capable of providing a lot of details about protein-protein interaction binding pattern more than binding affinity. To our knowledge, no one has systematically studied the details of antibody-antigen binding and mutant effects for NTD yet using computing methods. Herein, we pay attention to *in silico* approaches to explore the crucial residues for NTD-antibody binding and predict mutational implications for neutralizing effectiveness. Methodically analyzing binding patterns by molecular dynamics (MD) simulation and end-point molecular mechanics generalized Born surface area (MM/GBSA)²⁵ binding free energy calculation helps to shed light on the binding mechanisms of NTD-antibody. Our results revealed that mutations of some residues on NTD including Y144, K147, R246, Y248 have the high hazard of immune evasion for many antibodies and R246I mutation may reduce the efficacies of most current NTD antibodies through abolishing the hydrogen bond and electrostatic interaction with antibodies. Our research findings could be beneficial for drug design and mAbs-based therapeutics in clinical.

RESULTS AND DISCUSSION

Mapping the binding interface of S protein to 11 NTD antibodies

Taking the integrity of structures and the availability of biological experiment data into account, we have studied 11 systems consisting of diverse antibodies in this paper (Table S1 for details). Through mapping the interface residues on S protein NTD, we found that the interface includes about 40 residues, which are Y144, R246, Y145, H146, R158, T250, K147, Y248, L249, P251, D253, Q14, V16, N148, S247, G252, S254, S255, C15, N17, K150, W152, S256, V143, E156, L18, T19, G142, H245, G257, N74, T76, K77, F140, E154, L244, W258, G75, T20 and T73. These residues constitute antibodies' epitopes, which concentrate in N terminus (residue 14-19), a β -sheet spanning residue 144-158 and a loop formed by residue 246-256, collectively forming an antigenic site on the pinnacle of the NTD (Figure 1, red surface).

Binding interfaces of all 11 antibodies are highly overlapping and flanked by four oligosaccharides at position N17, N74, N122 and N149, which may exert an impact on

antibodies' binding.

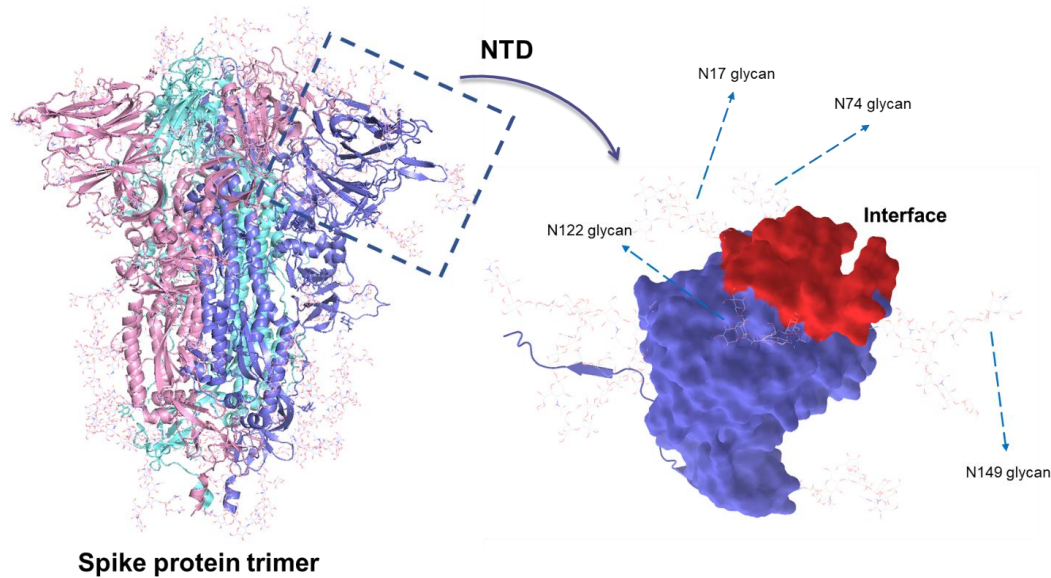


Figure 1. The binding interface of glyco-NTD to 11 antibodies. The left is S protein trimer with different colors for each chain and the right is a larger view of NTD. Glycans are shown as lines and the NTD is shown as surface. The red region represents the superimposed interfaces to 11 antibodies.

Key residues in NTD for neutralizing mAbs binding

We performed all-atom molecular dynamics simulation for 11 prototype glycosylated NTD-antibody systems, and the frames extracted from 30-60ns trajectories were applied to subsequent analysis. The key binding residues were identified from analysis of the MM/GBSA binding free energy decomposition results, and the residues with energy contribution < -1.00 kcal/mol were chosen as pivotal residues.

In total, there are 38 key residues in S protein NTD for all 11 systems (Figure 2A). The greater the energy contribution of the residues means that its mutations are more likely to affect the effectiveness of antibodies. As indicated in Figure 2A, R246 takes the most vital part in five systems *viz.* 5-24 (PDB ID: 7L2F), 4A8 (PDB ID: 7C2L), FC05 (PDB ID: 7CWS), 2-51 (PDB ID: 7L2C), 1-87 (PDB ID: 7L2D) (Figure 2A, Table S2). In the five systems, the energy contribution of R246 is over 9.90 kcal/mol (Table S2). Therefore, the mutations of R246 have the highest risk of immune escape. In addition, mutants of K147 may also affect the potencies of some antibodies. Research

results by McCallum *et.al* already showed that K147T mutant weakens the potencies of 4A8 (PDB ID: 7C2L), S2X333 (PDB ID: 7LXY) and S2M28 (PDB ID: 7LY2), but has little implication in S2L28 (PDB ID: 7LXZ)¹¹, which is in accordance with our prediction about K147 (Figure 2A).

When it comes to occupancy frequencies of key residues among 11 systems, there are 14 residues that have direct interaction with 3 or more antibodies, and 9 residues, concentrating in residues 144-147 and 246-252, that play an important role in 5 or more systems (Figure 2B). In particular, Y144 is involved in almost all mAbs binding except DH1052 (PDB ID: 7LAB), and the mutants of Y144 like Y144del and Y144F are already present in the real world²⁶. Y144, K147, R246 and Y248 make a relatively large contribution in 8 or more antibodies binding, hinting mutations of these four residues have the high possibility to affect binding affinities of most NTD mAbs. Thus, we should pay special attention to these sites when optimizing antibodies to NTD.

In consideration of both binding free energy contribution and occupancy frequency, R246 on S protein has the strongest binding affinity to the antibodies among the first four residues with the high frequency, arousing our interest to do further investigation.

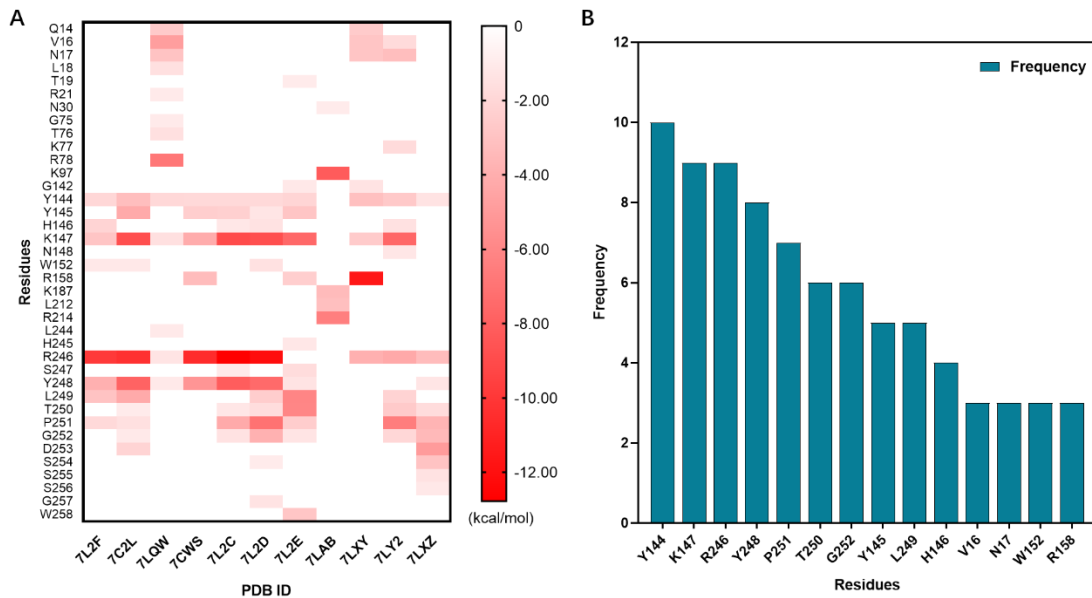


Figure 2. The key residues for NTD-antibody binding selected from NTD. (A) The heatmap of vital residues. The y axis presents the residues on NTD; the x axis presents PDB ID of different NTD-antibody complexes. The bar on the right represents the correlation between binding energy contribution and the color. (B) The occupancy

frequencies of key residues in all 11 systems.

Impact of R246I mutation on S protein for NTD-specific antibodies binding

In light of the research of Wibmer *et al.*, R246I has already appeared in SARS-CoV-2 Beta (B.1.351) variant¹³. To evaluate the binding affinity between various antibodies and R246I mutant NTD, MM/GBSA calculations were carried out with wild type NTD as control based on 2 independent MD runs lasting 60ns.

The results of binding free energy (ΔG) with glycans' contribution are hard to reproduce in each experiment (Table S3). In order to exploring more details, 500ns MD simulation was executed for 7L2F complex. As indicated in Figure S1, the three flexible sugars (N17, N74, N122 glycan), especially N17 glycan, move intensely and stay closed to the antibody within 3 angstroms most of the time for wild type complex (Figure S1A), while for R246I complex, the sugars are more than 5 angstroms away from the antibody in most of the time (Figure S1B). What's more, the energy contribution of glycans varies between -2.75 and -26.82 kcal/mol in the wild type complex, but only between -9.02 and 2.76 kcal/mol in the R246I mutant (Figure S1C). In conclusion, the flexibility of glycans allows their binding free energy contribution to vary greatly over time and have a big gap between the two systems. Whereas, provided that single point mutations don't cause large conformational changes, the contribution of sugars in the wild type and mutant should be similar. It's hard to sample statistically significant conformations of complexes with sugars at different positions over a limited period of simulation time. In this article we focus on the effect of residue mutations on antibody binding, rather than the role of sugars. Thus, when calculating binding affinities between NTD and antibodies, we excluded the contribution of sugars.

As shown in Figure 3 (Table S4 for details), ΔG of wild type NTD is higher than that of R246I mutant in 8 systems except for 4-18 (PDB ID: 7L2E), DH1052 (PDB ID: 7LAB), S2X333 (PDB ID: 7LXY), suggesting that R246I mutant has the potential to impact the effectiveness of these 8 antibodies. As was expected, the energy contribution changes of R246 and I246 to the overall binding energy show the same tendency as ΔG (Figure 4). Moreover, we performed 500ns MD simulation for 7L2F complex, whose

trends of $\Delta\Delta G$ in different length of simulation time are consistent with the result of 30-60ns (Table S5). This demonstrated that 60ns simulation is enough to obtain the variation tendency. Recent studies show that R246I can weaken the affinity of some antibodies, to varying degrees, including 5-24 (PDB ID:7L2F), 4A8 (PDB ID: 7C2L), 2-17 (PDB ID: 7LQW), FC05 (PDB ID: 7CWS)^{16,27}, and our predictions of percentage change in the relative binding free energy for above four systems are -53.76%, -40.58%, -13.92%, -19.13% respectively (Figure 3, Table S4). Therefore, our predicted trends of the relative binding free energy percentage are in good agreement with existing experimental findings, proving that our method is reliable to a certain extent.

According to our prediction, the percentage of relative binding free energy between wild type NTD and R246I mutant to antibodies are -28.85%, -16.95%, -13.87% and -13.72% for 1-87 (PDB ID:7L2D), 2-51 (PDB ID: 7L2C), S2M28 (PDB ID: 7LY2) and S2L28 (PDB ID:7LXZ) respectively, implying R246I mutation is possible to impair the efficacies of these four antibodies (Figure 3, Table S4). One of the most noteworthy things is that the affinity decreases the most for antibody 1-87 (PDB ID: 7L2D). These results suggest that it is best to avoid using these four types of antibodies alone, especially 1-87, against variants with R246I mutations. Moreover, the $\Delta\Delta G$ for 4-18 (PDB ID:7L2E), DH1052 (PDB ID:7LAB) and S2X333 (PDB ID:7LXY) are around 0 kcal/mol (Table S4), which is indicative of negligible impact on binding affinity (P value > 0.01). These three antibodies may not be susceptible to R246I mutation, so when targeting a mutant strain of SARS-COV-2 that has R246I mutation, they may work even better. Our findings can provide guidance on the clinical use of NTD antibodies.

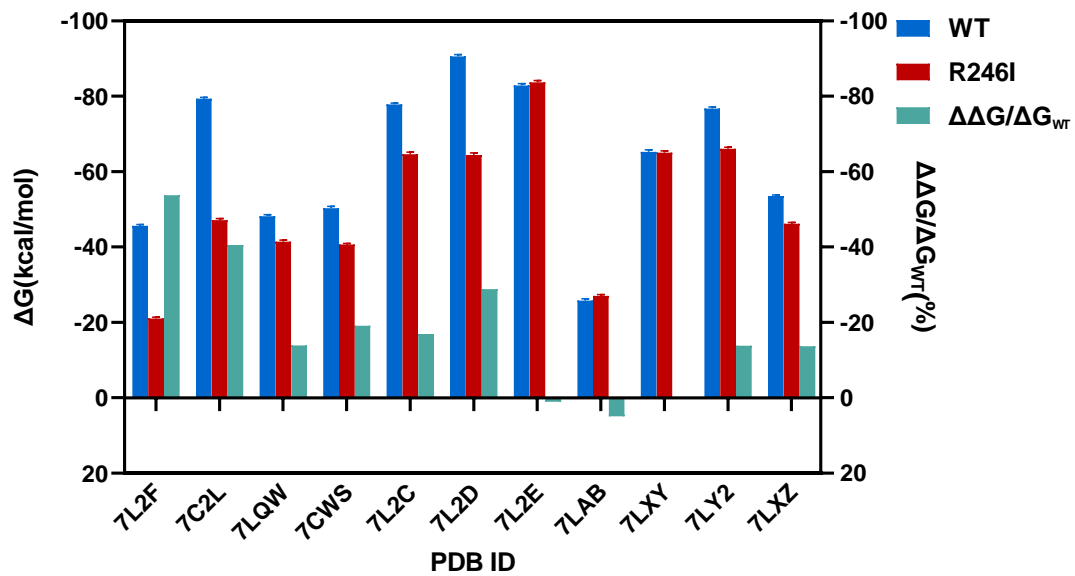


Figure 3. The binding free energy between prototype or R246I mutation NTD and mAbs. The binding free energy in WT is filled with blue, and the binding free energy in R246I mutant is filled with dark red. The relative binding free energy percentage ($\Delta\Delta G/\Delta G_{WT} = (\Delta G_{R246I} - \Delta G_{WT}) / \Delta G_{WT}$) between WT and R246I is filled with cyan.

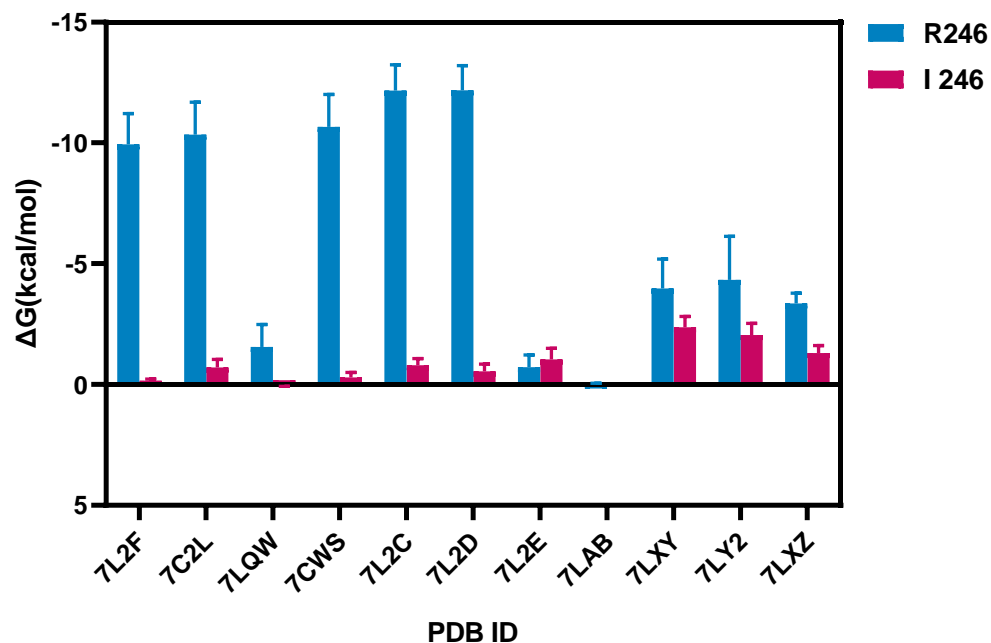


Figure 4. The contribution of R246 and I246 in 11 NTD-antibody systems. 251 snapshots from 30-60ns trajectories are used for per residue energy decomposition.

Molecular mechanism for 5-24 binding to R246I mutant NTD

In order to understand the underlying mechanism of R246I mutation, we carried out a more detailed analysis for the trajectory of glycosylated NTD-(5-24) complex (PDB ID: 7L2F). Through energy decomposition of per residue, we found that R246 has a large negative value (-9.95 ± 1.28 kcal/mol), while I246 has an energy contribution close to zero (-0.15 ± 0.07 kcal/mol), which illustrates I246 has much less contact with 5-24 compared with R246 (Figure 5A). What's more, the contribution of residue D105 in 5-24 tends to be reversed before and after the mutation (Figure 5A), suggesting that R246 are in close contact with D105.

Based on above results, we analyzed hydrogen bonds and electrostatic interaction between D105 in 5-24 and R246 or I246 in NTD in the 500ns MD production phase. Statistically, R246 has various amounts of stable hydrogen bonds with D105, which stabilizes at 2 hydrogen bonds and goes up to 3 sometimes (Figure 5B). However, I246 has no such interaction with antibody during all the simulation time (data not shown). As expected, the positively charged R246 forms a strong electrostatic interaction with D105, while R246I mutation with a neutral charge abolishes that interaction (Figure 5C). To further demonstrate the stability of the electrostatic interaction, we analyzed the distance between R246 and D105 during the whole simulation process. The distance between R246 and D105 is less than 3.75 Å during 92% of the simulation time, while I246 is more than 6.00 angstroms away from D105 all the time (Figure 5D), corroborating the idea that this interaction between R246 and D105 is very stable and intense.

It should be noticed that the phenomenon of hydrogen bonds and electrostatic interaction formed between R246 and antibody observed in the 7L2F is not unique. We noted that R246 in NTD is in close contact with glutamic acid in several antibodies, *viz* 4A8 (PDB ID: 7C2L), FC05 (PDB ID: 7CWS), 2-51 (PDB ID: 7L2C), 1-87 (PDB ID: 7L2D), with a mode similar to R246-D105 as highlighted in Figure S2. Because of the above reasons, R246I mutation will decrease the binding affinity to many antibodies.

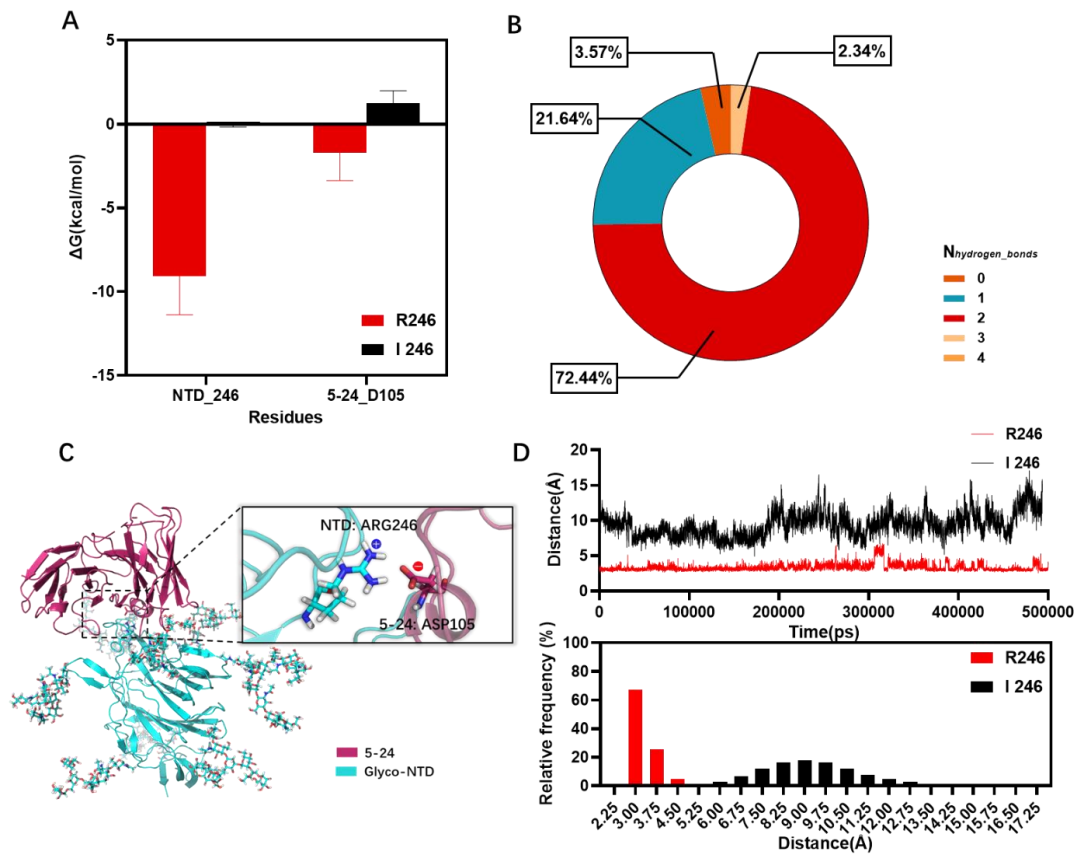


Figure 5. The changes in binding modes between NTD and antibody 5-24. (A) The energy contributions of residue 246 in NTD (red) and residue 105 (black) in antibody 5-24 in NTD_{WT}-(5-24) and NTD_{R246I}-(5-24), respectively. (B) The percentage of different numbers of hydrogen bonds in the whole 500ns simulation for prototype NTD-(5-24) complex. (C) Interactions of R246 (cyan) belonging to NTD and D105 belonging to antibody 5-24 (warm pink). The blue circular icon represents positive charge and the red one is negative charge. (D) the distances between D105 side chain in 5-24 and R246 (red) or I246 (black) in NTD and relative frequency distribution of the distances.

CONCLUSION

In the face of the severe epidemic of COVID-19, it is urgent to have a deep understanding of molecular mechanisms of harmful mutations and the vital antigenic epitopes when we are developing treatment and prevention methods. This paper applied a series of in silico methods to explore the binding patterns of different antibodies to S protein NTD. By per residue energy decomposition, some residues, including R246,

Y144, K147 and Y248, are found to play a crucial role in multiple NTD-specific antibodies binding. This result reminds us that mutations of these residues has the potential to cause immune evasion. By the means of MD simulation and MM/GBSA calculation, we predicted that R246I mutation may decrease or even invalidate the effectiveness of some mAbs. Further analysis of the molecular mechanism revealed that the immune escape of R246I mutation from 5-24 could be, to a great degree, attributed to the abolishment of the strong hydrogen bonds and electrostatic attractions between R246 of NTD and D105 of antibody. The findings in this study makes it possible to optimize existing therapeutic antibodies, thus making them more efficacious against COVID-19.

EXPERIMENTAL SECTION

Preparation of mAb-S protein complexes

As of May 1, 2021, we have retrieved 14 NTD-specific antibodies bound to S protein from the Protein Data Bank. Considering the integrity of structures and the availability of biological experiment data, we have studied 11 systems in this paper. The NTD domain (residue 14 or 27-291) were truncated from the full-length S protein and both terminals are capped with ACE and NME, respectively. In order to get an intact structure, missing residues in flexible loops were modeled using SWISS-MODEL²⁸⁻²⁹. The interfaces analysis was carried out using scripts of pymol2.5³⁰ with a cutoff of 0.75. Glycosylated NTD wild type and R246I mutation models were generated using *Glycan Reader* module³¹⁻³³ available within CHARMM-GUI³⁴ according to Table S6.

System preparation

Protonation states were assessed using H++ 3.2³⁵⁻³⁶ at pH 7.4. A cubic explicit water box described using the TIP3P model was used to solvated the complex system, which was extended by 12 Å from the solute. An atmosphere of 150 mM NaCl was also included in all simulations. The generated models were parametrized using CHARMM36 all-atom additive force fields for protein and glycans³⁷⁻³⁸. 8,000 steps of

minimization including 6,000 steps of steepest descent minimization and 2,000 steps of conjugate gradient minimization were performed to remove bad contacts during the energy minimization phase. Subsequently, the temperature was incrementally changed from 0 to 300 K for 125ps at 1 fs/step. Equilibration in NPT ensemble was run at 1.0 bar and 300 K for 500,000 steps at 2fs/step. Pmemd program implement in Amber18 software package³⁹ was used to run the minimization, heating simulations with position constraints (1 kcal/mol/Å²) on protein and dihedral Angle constraints on carbohydrates.

Molecular dynamics (MD) simulations

Pmemd.cuda in Amber18 was used to perform MD simulations at 300 K, 1 bar for all NTD-antibody complexes. Temperature and pressure were controlled by Langevin thermostat⁴⁰ and a Nosé-Hoover Langevin barostat⁴¹⁻⁴². Bonds involving hydrogen atoms were fixed by the SHAKE algorithm⁴³. The cutoff distance applied for van der Waals interactions was 12 Å. All simulations were performed using particle-mesh Ewald (PME) for long-range electrostatic interactions⁴⁴. Cpptraj module in Amber18 was used for trajectory processing.

Binding free energy calculation

Binding free energy (ΔG) of NTD-antibody complexes was calculated by MM/GBSA method²⁵ using GB OBC model (igb=2) with a salt concentration of 150 mM. In this study, the internal and external dielectric constants were set to 1.0 and 78.5 separately. When calculating the binding affinity excluding glycans' contribution, we made use of Amber18 built-in program Cpptraj to remove glycans in every trajectory, and pymol2.5³⁰ to add hydrogens for glycosylation sites. The free energy decomposition analysis was carried out using an internal program with idecomp=1.

ACKNOWLEDGMENTS

This work was supported by the Natural Science Foundation of Shanghai (21ZR1475600) and National Key R&D Program of China (2016YFA0502301 & 2017YFB0202601). The simulations were partially run at the TianHe 1 supercomputer in Tianjin and TianHe 2 supercomputer in Guangzhou.

REFERENCES

1. Who Coronavirus (Covid-19) Dashboard. <https://covid19.who.int/>. (26 August 2021, date last accessed).
2. Dhama, K.; Khan, S.; Tiwari, R.; Sircar, S.; Bhat, S.; Malik, Y. S.; Singh, K. P.; Chaicumpa, W.; Bonilla-Aldana, D. K.; Rodriguez-Morales, A. J., Coronavirus Disease 2019-Covid-19. *Clin Microbiol Rev* **2020**, *33*.
3. Lu, R., et al., Genomic Characterisation and Epidemiology of 2019 Novel Coronavirus: Implications for Virus Origins and Receptor Binding. *Lancet* **2020**, *395*, 565-574.
4. Wan, Y.; Shang, J.; Graham, R.; Baric, R. S.; Li, F., Receptor Recognition by the Novel Coronavirus from Wuhan: An Analysis Based on Decade-Long Structural Studies of Sars Coronavirus. *J Virol* **2020**, *94*.
5. Tortorici, M. A.; Veessler, D., Structural Insights into Coronavirus Entry. *Adv Virus Res* **2019**, *105*, 93-116.
6. Walls, A. C.; Park, Y. J.; Tortorici, M. A.; Wall, A.; McGuire, A. T.; Veessler, D., Structure, Function, and Antigenicity of the Sars-Cov-2 Spike Glycoprotein. *Cell* **2020**, *183*, 1735.
7. Hansen, J., et al., Studies in Humanized Mice and Convalescent Humans Yield a Sars-Cov-2 Antibody Cocktail. *Science* **2020**, *369*, 1010-1014.
8. Tortorici, M. A., et al., Ultrapotent Human Antibodies Protect against Sars-Cov-2 Challenge Via Multiple Mechanisms. *Science* **2020**, *370*, 950-957.
9. Cerutti, G., et al., Potent Sars-Cov-2 Neutralizing Antibodies Directed against Spike N-Terminal Domain Target a Single Supersite. *Cell Host Microbe* **2021**, *29*, 819-833.e7.
10. Chi, X., et al., A Neutralizing Human Antibody Binds to the N-Terminal Domain of the Spike Protein of Sars-Cov-2. *Science* **2020**, *369*, 650-655.
11. McCallum, M., et al., N-Terminal Domain Antigenic Mapping Reveals a Site of Vulnerability for Sars-Cov-2. *Cell* **2021**, *184*, 2332-2347.e16.
12. McCarthy, K. R.; Rennick, L. J.; Nambulli, S.; Robinson-McCarthy, L. R.; Bain, W. G.; Haidar, G.; Duprex, W. P., Recurrent Deletions in the Sars-Cov-2 Spike Glycoprotein Drive Antibody Escape. *Science* **2021**, *371*, 1139-1142.
13. Harvey, W. T., et al., Sars-Cov-2 Variants, Spike Mutations and Immune Escape. *Nat Rev Microbiol* **2021**, *19*, 409-424.
14. Greaney, A. J., et al., Complete Mapping of Mutations to the Sars-Cov-2 Spike Receptor-Binding Domain That Escape Antibody Recognition. *Cell Host Microbe* **2021**, *29*, 44-57 e9.
15. Wibmer, C. K., et al., Sars-Cov-2 501y.V2 Escapes Neutralization by South African Covid-19 Donor Plasma. *Nat Med* **2021**, *27*, 622-625.
16. Wang, P., et al., Antibody Resistance of Sars-Cov-2 Variants B.1.351 and B.1.1.7.
17. Kimura, I., et al., Sars-Cov-2 Lambda Variant Exhibits Higher Infectivity and Immune Resistance. *bioRxiv* **2021**, 2021.07.28.454085.
18. Verma, J.; Subbarao, N., Insilico Study on the Effect of Sars-Cov-2 Rbd Hotspot Mutants' Interaction with Ace2 to Understand the Binding Affinity and Stability. *Virology* **2021**, *561*, 107-116.
19. Shah, M.; Ahmad, B.; Choi, S.; Woo, H. G., Mutations in the Sars-Cov-2 Spike Rbd Are Responsible for Stronger Ace2 Binding and Poor Anti-Sars-Cov Mabs Cross-Neutralization. *Computational and Structural Biotechnology Journal* **2020**, *18*, 3402-3414.

20. Smaoui, M. R.; Yahyaoui, H., Unraveling the Stability Landscape of Mutations in the Sars-Cov-2 Receptor-Binding Domain.
21. Luan, B.; Huynh, T., Insights into Sars-Cov-2's Mutations for Evading Human Antibodies: Sacrifice and Survival. *J. Med. Chem.* **2021**.
22. Luan, B.; Wang, H.; Huynh, T., Enhanced Binding of the N501y-Mutated Sars-Cov-2 Spike Protein to the Human Ace2 Receptor: Insights from Molecular Dynamics Simulations. *FEBS Lett* **2021**, 595, 1454-1461.
23. Wu L, P. C., Xu Z, Zhu weiliang, Predicting the Potential Effect of E484k Mutation on the Binding of 28 Antibodies to the Spike Protein of Sars-Cov-2 by Molecular Dynamics Simulation and Free Energy Calculation. *ChemRxiv* **2021**.
24. Elbe, S.; Buckland-Merrett, G., Data, Disease and Diplomacy: Gisaid's Innovative Contribution to Global Health. *Glob Chall* **2017**, 1, 33-46.
25. Kollman, P. A., et al., Calculating Structures and Free Energies of Complex Molecules: Combining Molecular Mechanics and Continuum Models. *Acc Chem Res* **2000**, 33, 889-97.
26. Korber, B., et al., Tracking Changes in Sars-Cov-2 Spike: Evidence That D614g Increases Infectivity of the Covid-19 Virus. *Cell* **2020**, 182, 812-827.e19.
27. Sun, Y., et al., Structure-Based Development of Three- and Four-Antibody Cocktails against Sars-Cov-2 Via Multiple Mechanisms. *Cell Res* **2021**, 31, 597-600.
28. Bertoni, M.; Kiefer, F.; Biasini, M.; Bordoli, L.; Schwede, T., Modeling Protein Quaternary Structure of Homo- and Hetero-Oligomers Beyond Binary Interactions by Homology. *Sci Rep* **2017**, 7, 10480.
29. Waterhouse, A., et al., Swiss-Model: Homology Modelling of Protein Structures and Complexes. *Nucleic Acids Res.* **2018**, 46, W296-W303.
30. Schrödinger, L., The Pymol Molecular Graphics System, Version 2.5. 2021.
31. Jo, S.; Song, K. C.; Desaire, H.; MacKerell, A. D., Jr.; Im, W., Glycan Reader: Automated Sugar Identification and Simulation Preparation for Carbohydrates and Glycoproteins. *J Comput Chem* **2011**, 32, 3135-41.
32. Park, S. J.; Lee, J.; Patel, D. S.; Ma, H.; Lee, H. S.; Jo, S.; Im, W., Glycan Reader Is Improved to Recognize Most Sugar Types and Chemical Modifications in the Protein Data Bank. *Bioinformatics* **2017**, 33, 3051-3057.
33. Park, S. J.; Lee, J.; Qi, Y.; Kern, N. R.; Lee, H. S.; Jo, S.; Jung, I.; Joo, K.; Lee, J.; Im, W., Charmm-Gui Glycan Modeler for Modeling and Simulation of Carbohydrates and Glycoconjugates. *Glycobiology* **2019**, 29, 320-331.
34. Warren, T. K., et al., Therapeutic Efficacy of the Small Molecule Gs-5734 against Ebola Virus in Rhesus Monkeys. *Nature* **2016**, 531, 381-5.
35. H++, <http://biophysics.cs.vt.edu/H++>.
36. Anandkrishnan, R.; Aguilar, B.; Onufriev, A. V., H++ 3.0: Automating Pk Prediction and the Preparation of Biomolecular Structures for Atomistic Molecular Modeling and Simulations. *Nucleic Acids Res* **2012**, 40, W537-41.
37. Huang, J.; MacKerell, A. D., Jr., Charmm36 All-Atom Additive Protein Force Field: Validation Based on Comparison to Nmr Data. *J Comput Chem* **2013**, 34, 2135-45.
38. Guvench, O.; Hatcher, E. R.; Venable, R. M.; Pastor, R. W.; Mackerell, A. D., Charmm Additive All-Atom Force Field for Glycosidic Linkages between Hexopyranoses. *J Chem Theory Comput* **2009**, 5, 2353-2370.

39. D.A. Case, H. M. A., K. Belfon, I.Y. Ben-Shalom, S.R. Brozell, D.S. Cerutti, T.E. Cheatham, III, V.W.D. Cruzeiro, T.A. Darden, R.E. Duke, G. Giambasu, M.K. Gilson, H. Gohlke, A.W. Goetz, R. Harris, S. Izadi, S.A. Izmailov, C. Jin, K. Kasavajhala, M.C. Kaymak, E. King, A. Kovalenko, T. Kurtzman, T.S. Lee, S. LeGrand, P. Li, C. Lin, J. Liu, T. Luchko, R. Luo, M. Machado, V. Man, M. Manathunga, K.M. Merz, Y. Miao, O. Mikhailovskii, G. Monard, H. Nguyen, K.A. O’Hearn, A. Onufriev, F. Pan, S. Pantano, R. Qi, A. Rahnamoun, D.R. Roe, A. Roitberg, C. Sagui, S. Schott-Verdugo, J. Shen, C.L. Simmerling, N.R. Skrynnikov, J. Smith, J. Swails, R.C. Walker, J. Wang, H. Wei, R.M. Wolf, X. Wu, Y. Xue, D.M. York, S. Zhao, and P.A. Kollman *Amber 2018*, University of California, San Francisco, 2018.
40. Ermak, D. L.; McCammon, J. A., Brownian Dynamics with Hydrodynamic Interactions. *The Journal of Chemical Physics* **1978**, *69*, 1352-1360.
41. Martyna, G. J.; Tobias, D. J.; Klein, M. L., Constant Pressure Molecular Dynamics Algorithms. *The Journal of Chemical Physics* **1994**, *101*, 4177-4189.
42. Feller, S. E.; Zhang, Y.; Pastor, R. W.; Brooks, B. R., Constant Pressure Molecular Dynamics Simulation: The Langevin Piston Method. *The Journal of Chemical Physics* **1995**, *103*, 4613-4621.
43. Ryckaert, J.-P.; Ciccotti, G.; Berendsen, H. J. C., Numerical Integration of the Cartesian Equations of Motion of a System with Constraints: Molecular Dynamics of N-Alkanes. *Journal of Computational Physics* **1977**, *23*, 327-341.
44. Essmann, U.; Perera, L.; Berkowitz, M. L.; Darden, T.; Lee, H.; Pedersen, L. G., A Smooth Particle Mesh Ewald Method. *The Journal of Chemical Physics* **1995**, *103*, 8577-8593.